American Journal of Environmental Sciences 4 (5): 420-438, 2008
ISSN 1553-345X

Using a Simulation Tool to Model the Ground Level Concentrations of Green House Gases Emitted by Flaring in Petroleum Production in Kuwait Oilfields

[1]Khaireyah Kh. AL-Hamad, [1]V. Nassehi and [2]A.R. Khan
[1]Department of Chemical Engineering,
Loughborough University, Leicestershire, LE11 3TU, UK
[2]Coastal and Air Pollution Division, Kuwait Institute for Scientific Research
P.O. Box 24885, Safat 13109, Kuwait

Abstract: Air pollution and its effects on the ecosystem has been a source of concern for many environmental pollution organizations in the world. In particular climatologists who are not directly involved in petroleum industry sometimes express concerns about the environmental impacts of gas emissions from flaring at well heads. For environmental and resource conservation reasons, flaring should always be minimized as much as practicable and consistent with safety considerations. However, any level of flaring has a local environmental impact, as well as producing emissions which have the potential to contribute to the global warming. In the present research the Industrial Source Complex (ISCST3) Dispersion Model is used to calculate the ground level concentrations of two selected primary pollutants (i.e. methane and non-methane hydrocarbons) emitted due to flaring in all of Kuwait Oilfields. In additional, the performance of the ISCST3 model is assessed, by comparing the model prediction with the observed concentration of methane and non-methane hydrocarbons obtained from the monitoring sites. The described model evaluation is based on the comparison of 50 highest daily measured and predicted concentrations of methane and non-methane hydrocarbons. The overall conclusion of this comparison is that the model predictions are in good agreement with the observed data (accuracy range of 60-95%) from the monitoring stations maintained by the Kuwait Environmental Public Authority (EPA). A specific important conclusion of this study is that, there is a need for a proper emission inventory strategy for Kuwait Oil Company (KOC) as means of monitoring and minimizing the impact of methane and non-methane hydrocarbons released because of flaring activities.

Key words: Kuwait oilfields, ISCST3 model, flare activities, Kuwait-EPA monitoring station

INTRODUCTION

Kuwait is a major oil exporting country and its economy, growth and prosperity is heavily dependent on oil production. KOC is at the heart of the petroleum production in Kuwait. The oilfields involve various types of industrial operations and activities, such as drilling, production of crude oil, fuel combustion and flaring of gases which all result in gas emission into atmosphere. In practice, all other sources of emissions are small compared with emissions from flaring. Consequently, a wide range of air pollutant emissions is generated on various sites. Such emissions include carbon dioxide, nitrogen and sulfur oxide gases, methane and non-methane hydrocarbons and suspended particulates.

A comprehensive impact assessment study has been previously published[1] which provides an account and estimates of all emissions of primary pollutants associated from flaring activities in the Kuwait Oilfields. This inventory records the annual emissions of air pollutants: NO_X, SO_2, CO, CO_2, methane and non-methane hydrocarbons. The emissions are generated from various point sources and aggregated to obtain total pollutants load of ambient air. The emissions of pollutants from the flaring associated with all types of operations in the oilfields, Gathering Centers (GC), Booster Stations (BS), tank areas and other oil production related activities.

In the present research the previously published data are used as the necessary input for the ISCST3 model. Obviously methane and non-methane hydrocarbons are not the only green house gasses which result from flaring activities.

However these gases provide a typical sample which can be used as an input for the ISCST3 model to

Corresponding Author: Khaireyah Kh. AL-Hamad, Department of Chemical Engineering, Loughborough University, Leicestershire, LE11 3TU, UK

investigate of the effects of gases emitted from flaring in all of Kuwait Oilfields.

EPA MONITORING STATIONS IN THE STATE OF KUWAIT

Kuwait EPA has established a number of fixed monitoring stations to collect air quality data in the urban areas. These stations continuously measure the levels of pollutants such as SO_2, NO_2, CO, NO, CO_2, H_2S, O_3 and TSP (total suspended particles) in the air. In additional, the hourly air pollutants concentrations are measured continuously by fixed ambient air stations located over the State of Kuwait.

It is important to note that, in general, all of the monitoring stations are considered as urban stations distributed within the residential areas except for Um Al-Aish station, which is located in the northern part of the country far away from the residential areas. Fig. 1 shows the area map and the locations of Kuwait-EPA air quality monitoring sites. These monitoring stations are equipped with an automatic analyzer and meteorological sensors.

In order to assess the air quality in Kuwait, measurement of the concentrations of pollutants are collected from the Kuwait-EPA air quality-monitoring network. These concentration values of methane and non-methane hydrocarbons are analyzed and compared with the specified limits and guidelines published by the EPA and the model predictions for the ground level concentrations of methane and non-methane hydrocarbons from flaring in Kuwait Oilfields.

Fig. 1: Location of the air quality monitoring network in the state of Kuwait.

DESCRIPTION OF THE GEOGRAPHY AND METEOROLOGICAL CONDITIONS IN THE STATE OF KUWAIT

Geography of Kuwait: Kuwait has a small area of about 17,818 km^2. At its most distant points, it is about 200 km north to south and 170 km east to west.

Kuwait is shaped roughly like a triangle, surrounded by land on its northern, western and southern sides and sea on its eastern side, with 195 km of coastlines. The bulk of the Kuwaiti populations live in the coastal capital city of Kuwait. Smaller populations inhabit the nearby city of Al-Jahrah. Kuwait's land is mostly flat and arid with little or no ground water.

Meteorological conditions in Kuwait: Kuwait has a typical desert climate, hot and dry most of the time. Rainfall varies from seventy five to 150 mm a year across the country, however, rainfall ranging from twenty-five mm a year to as much as 325 mm have also been recorded.

In summer, average daily temperatures range from 42-46°C, the highest recorded temperature has been 51.5°C. The summers are relentlessly long, punctuated mainly by dramatic dust storms in June and July when northwesterly winds cover the cities in sand. In late summer, which is more humid, there are occasional sharp, brief thunderstorms.

Starting from November colder winter weather sets in temperatures dropping as low as 0°C at nights; daytime temperature remains in the 15-20°C range. Frost rarely occurs; rain is more common and falls mostly in the winter and spring.

Winters (November through February) are cool with some precipitation and average temperatures around 13°C (56°F) with extremes from 2-27°C. The spring season (March) is warm and pleasant with occasional thunderstorms. Surface coastal water temperatures range from 15°C (59°F) in February to 35°C (95°F) in August. The winter months are often pleasant, featuring some of the region's coolest weather, with daytime temperatures hovering around 18°C (64°F) and nights being genuinely chilly. Sandstorms occur throughout the year but are particularly common in spring.

State of Kuwait meteorological and data analysis for the year 2006: The meteorological conditions play a major role in the dispersion of the pollutions over the State of Kuwait. Therefore, the aim here is to report on

real meteorological conditions measured and recorded so that a clear picture can be drown about the climate in the state of Kuwait and its affect on the air pollution.

In order to use the meteorological data as input in the ISCST3 model a pre-processing program based on the US EPA. PCRAMMET is utilized to convert the Kuwait data into a suitable format.

A one year hourly record of the surface and upper air meteorological data for year 2006 obtained from the Kuwait International Airport (KIA) weather station is used in the present study for simulation of the dispersion of methane and non-methane hydrocarbons emitted from flaring in all Kuwait Oilfields areas (NK, SEK, WK).

One of the main meteorological factors that can affect the behavior of the pollutants trends during a day is the mixing height and depth of the mixing layer. US-EPA[2,3,4] stated that the estimation of mixing heights from upper air meteorological data is a critical parameter for understanding the formation, dispersion and transfer of ozone and precursors during pollution episodes. The upper air meteorological data were obtained from routine measurements at the KIA weather station for the year 2006. These data were used to calculate the mixing heights (Fig. 2.) and investigate the effects of upper air meteorological data in the diurnal behaviors of ozone and its precursors.

The morning and afternoon mixing height estimates are determined based on the method described by Holzworth[5] and Hanna[6]. Mixing height is estimated by plotting maximum surface temperature and drawing a line parallel to the dry adiabatic lapse rate from the point of maximum surface temperature to point at which the line intersects the ambient lapse rate early morning as shown in Fig. 2.

The prevailing wind direction in Kuwait is along the north westerly quadrant throughout the year, but it is more so in summer. Figure 3a and 3b show detailed wind rose plots for the year 2006 and the main two seasons in Kuwait.

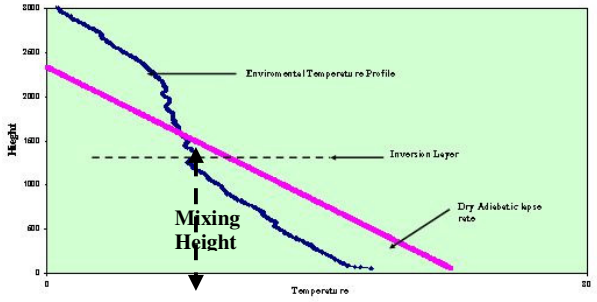

Fig. 2: Upper air temperature profile and formation of the temperature inversion

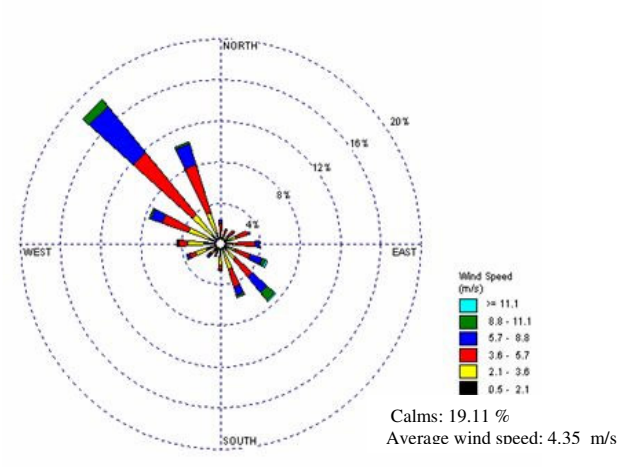

Fig. 3a: Wind rose plot for winter (November-March)

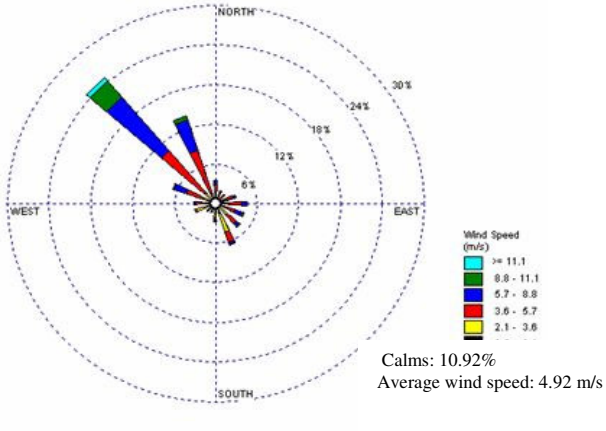

Fig. 3b: Wind rose plot for summer (April-October)

about 14.3% of the total time and an average wind speed of 4.7 m sec^{-1}. Figure 3a shows the wind rose plot for the winter (November-March) where most of the time the prevailing wind direction is from the North West with calm conditions about 19.11% of the total time and an average wind speed of 4.35 m sec^{-1}. Figure 3b provides the wind rose plot for summer (April-October) and shows that the prevailing wind direction is also from the North West. This indicates that there no marked seasonal variation in the wind direction throughout the year. The prevailing wind direction in summer is more established than winter season with calm wind 10.92% of the total time and an average wind speed of 4.92 m sec^{-1}. Moreover, there is no significant diurnal variation in the prevailing wind direction during the day and night times. This tends to minimize the effects of any land or sea breeze in the

dispersion of the pollutants in the urban areas of Kuwait.

The most important meteorological element that can control the level of the atmospheric pollution is the wind. The wind in the state of Kuwait results from the influence of the pressure systems, which dominate the area during each season.

In Fig. 4, the frequency distribution of the winds is illustrated. There are about 32.2% of wind speed record is in between 3.6-5.7 m sec^{-1} and about 17.5% of wind speed record in between 2.1-3.6 m s^{-1}. As shows in detailed wind rose plots (Fig. 3, a and b), the main prevailing wind direction in NW is more frequent than other directions (i.e., N, NNW and W). In addition, it can be noted that the North West wind direction coincides with high wind speeds than other directions.

The effect of the wind speed is a very important parameter in the dispersion of pollutants as the relationships between the wind speed and the concentration of pollutants downwind of a source is of inversely proportional. This means that when the wind speed reaches its highest level it actually helps in reducing the concentration of any air pollution, thus reducing its hazardous effects on the residential area. On the other hand, slow winds allow for high concentration of pollutants moving slowly over residential areas.

Table 1 shows the Mean Monthly Wind Speed (MMWS) and the Mean Monthly Ambient Temperature (MMAT) for 2006. These mean monthly meteorological data were computed from the hourly records during each day of 2006. The annual mean wind speed in 2006 is low being only 4.04 m sec^{-1}, while MMWS reaches its highest in June (5.23 m sec^{-1}) and in July (6.07 m sec^{-1}) and its lowest in January (3.18 m sec^{-1}). The annual mean temperature was 27.07°C where the lowest MMAT recorded during the year was 11.61°C in December and the highest MMAT was 40.04°C in July. This variation of temperature and wind speeds may have serious consequences on determining the level of air pollution and hence the air quality, especially in residential areas closes to KOC Oilfields.

Table 1: Mean Monthly Meteorological Conditions for year 2006

Month	Mean wind speed (m sec^{-1})	Mean ambient temperature (°C)
January	3.18	13.50
February	3.73	15.94
March	4.10	21.17
April	4.01	26.30
May	4.27	34.25
June	5.23	38.52
July	6.07	40.04
August	3.75	39.34
September	3.66	34.41
October	3.76	30.18
November	3.43	19.58
December	3.33	11.61
Average	4.04	27.07

Figure 5 shows the MMAT, maximum and minimum temperatures recorded for each month. The maximum temperature in summer ranges from 40-51°C.

Table 2 shows the frequency distribution count for the wind direction under a specify winds speed class in 2006. The frequency of the calm winds was 14.3% of the 8736 hourly record data. In meteorology, the wind direction considered as the direction from which the wind is bellows therefore, a North West (NW) wind will move pollutants to the South East (SE) of the source. Hence, this consideration was taken into account in a construction of Table 1 and the wind rose plot shown in Fig. 3 to make the analysis of the wind

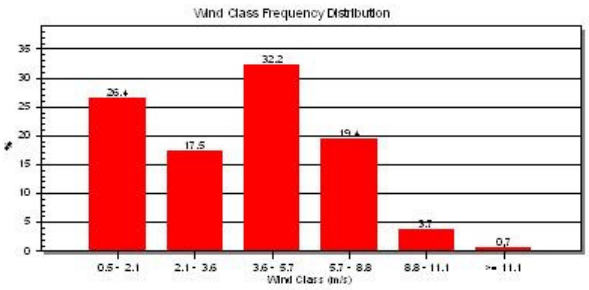

Fig. 4: Frequency Distribution of the Wind Speed Class during the year 2006

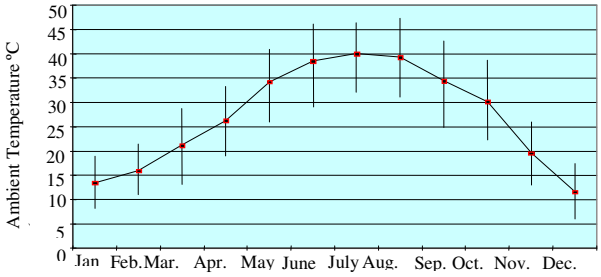

Fig. 5: The mean monthly, maximum and minimum record of ambient air temperature for year 2006

Table 2: Frequency distribution counts for the wind direction in year 2006

Wind direction	Wind speed class in (m sec^{-1}) 0.5-2.1	2.1-3.6	3.6-5.7	5.7-8.8	8.8-11.1	> = 11.1	Total
N	33	43	144	47	0	0	267
NNE	21	54	74	10	0	0	159
NE	30	40	85	6	1	0	162
ENE	32	61	154	28	0	0	275
E	35	82	204	60	1	0	382
ENE	34	79	156	106	25	5	405
SE	77	122	161	106	42	6	514
SSE	126	205	150	48	8	2	539
S	97	95	35	11	2	0	240
SSW	59	38	21	12	1	0	131
SW	69	36	31	23	2	0	161
WSW	132	112	42	9	1	0	296
W	114	109	77	20	0	3	323
WNW	76	132	247	136	17	2	610
NW	78	174	697	753	193	38	1933
NNW	47	144	536	324	33	6	1090
Total	1060	1526	2814	1699	326	62	7487

Frequency of calm winds: 14.3%; Calm wind h: 1249; Average wind speed: 4.70 m sec^{-1}

data more consistencies with the modeling results. However, it is very important to note that the ISCST3 model considers the wind direction as the direction towards which the wind is blowing.

MATHEMATICAL MODEL

Industrial Source Complex (ISCST3) dispersion model modified by the US EPA in 1999 is used in the present study. The ISCST3 algorithm is based on a Gaussian plume dispersion model (i.e., it solves the steady-state Gaussian plume equation) and calculates short-term pollutant concentrations from multiple point sources at a specified receptor grid on a level or gently sloping terrain. The ISCST3 model includes a wide range of options for modeling air quality impacts of pollution sources, making it a popular choice for the modeling community is a variety of applications.

Since the ISCST3 model is specially designed to support the US EPA's regulatory model programs[3,4], the regulatory modeling options, as specified in the revised guidelines for air quality models (USA-EPA, 1999), are the default mode of operation for the models. These options include the use of stack-tip downwash, buoyancy-induced dispersion, final plume rise, a routine for processing averages when calm winds prevail, default values for wind profile exponents and for the vertical potential temperature gradients and the use of upper bound estimates for super squat buildings having an influence on the lateral dispersion of the plume.

The model is capable of handling multiple sources, including point, volume, area and open pit source types. Line sources may also be modeled as a string of volume sources or as elongated area sources. Several source groups may be specified in a single run, with the source contributions combined for each group.

The ISCST3 model implementation requires three main inputs data as follows:

Source information: The source parameters required for the ISCST3 numerical model are pollutant emission rate (g sec^{-1}), location coordinates (UTM), source height (m), exit inner diameter (m), exit gas speed (m sec^{-1}) and exit gas temperature (°C). All the required information on the location coordinates, the emission rates and heights of stacks, diameters, speeds and temperatures of the gas flow at the exits of the stacks were collected from flaring activities from Kuwait oil field as stated in previous published.

Receptor information: The ISCST3 model have considerable flexibility in the specification of receptor locations, has the capability of specifying multiple receptor networks in a single run and may also mix Cartesian grid receptor networks and polar grid receptor networks in the same run.

Two different kinds of Cartesian coordinate receptors were used as an input to the ISCST3 model, these are:

- The uniform grid system of 441 receptors which cover approximately 55 by 53 km. The grid base elements is a square with side length of 1 km. Figure 6 describes one plot figure of the grid under study
- Discrete Receptors points corresponding to the location of the major pollution centers and the existing monitoring stations in the State of Kuwait. This means that concentrations in each point in the grid, which is 1km, will be estimated in addition to the discrete point of the existing monitoring stations. The matrix of concentrations can be plotted as a contour map for the selected meteorological data file

Indeed, the uniform grid receptors are not need for the model evaluation, neither for investigation of the efficiency of the monitoring sites, but it is a way to have a general view of the pollutants dispersion over the study area.

These receptors are selected based on actual sites in UTM location coordinate of Kuwait map as shown in Fig. 6.

Meteorological information: The meteorological data required are anemometer height (m) wind speed (v), wind direction (degree) clockwise from the north, air temperature, total and opaque cloud cover (%), stability class at the hour of measurement (dimensionless) and mixing height (m). The anemometer height, wind speed, wind direction, air temperature and cloud cover are usually obtained from direct measurements.

The hourly stability class and the hourly mixing height are estimated using PCRAMMET. PCRAMMET is a meteorological pre-processor for preparing National Weather Service (NWS) data for use in the ISCST3 US-EPA. The routine measurements of the surface and upper air meteorological data obtained from KIA for the year 2006 is used to run the PCRAMMET to generate an hourly ASCII input meteorological file containing the meteorological information parameters needed for the running of the ISCST3 model.

Fig. 6: The one grid area under study

The anemometer height of this station is 10 m. The average hourly meteorological data for 2006 were assumed to be valid for the periods investigated

The stability class was defined on the basis of Pasquill categories, which are mainly a function of the hour of measurement, wind speed and sky cover (i.e., the amount of clouds). Based on temperature profile measurements, the mixing height was estimated by the model.

DESCRIPTION OF THE STUDY AREA

The subject area of the present study covers all of the Kuwait's oil producing zones which are located in three selections in the state of Kuwait (Fig. 7). Figure 7 shows the Kuwait map with the location of the three oil producing areas (SEK, WK and NK) and the location of the residential areas.

The distance between the farthest northeast and southeast points of the state boundaries is about 200 Km and from farthest east to west is about 170 Km. Therefore, the total length of the border line is about 685 Km. To cover all of this area, modeling is divided into three individual tasks to calculate the ground level concentrations of methane and non-methane hydrocarbons. The modeling tasks are:

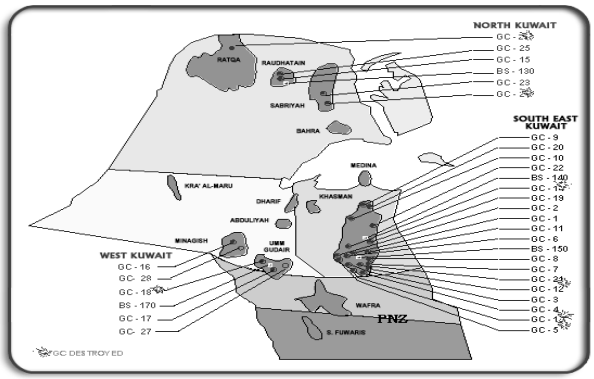

Fig. 7: Major oilfields and gathering Center (GC) in the state of kuwait

SouthEast Kuwait (SEK) area: Calculated greater Burgan area located in SEK, which has 14 gathering centers.

West Kuwait (WK) area: Calculated Minagish and Umm Gudair fields located in WK have 4 GCs and two BS's.

North Kuwait (NK) area: Calculated Ratqa, Raudatin and Sabiriyah which located in NK have 3 GCs and one BS.

RESULTS AND DISCUSSIONS

ISCST3 model was set up to simulate the ground level concentrations of methane and non-methane hydrocarbons emitted from flaring activities in KOC at all points covered by the receptors information. Modeling was then carried out by summing the steady state concentration contributions from each source at each receptor point in the study area. The calculations were done based on the model input parameters as described in the previous sections. The simulated results of the emission scenarios using the ISCST3 are

on an hourly basis for the predicted concentrations of methane and non-methane hydrocarbons.

The hourly, daily and annual average maximum ground level concentrations of methane and non-methane hydrocarbons were predicted and output results were compared with Kuwait Ambient Air Quality Standards (KAAQS) at all of the grid point receptors under the study area (443 receptors) as shown in Fig. 6. The maximum hourly, daily and annual Allowable levels of pollutants specified by KAAQS are shown in Table 3. The maximum hourly level as indicated by KAAQS can be exceeded only once a month during a year in the same location. However, the daily and annually allowable limits are not to be exceeded.

North Kuwait oilfield area results

Methane emission: Table 4a-c show the modeling results for the 50 highest hourly, 50 highest daily and the 50 highest annual maximum ground level

Table 3: Kuwait EPA standards for ambient air

		Standards			
Pollutants	Units	Annual	24 h	8 h	Hourly
NO_2	ppb	30 (67 μg m^{-3})	50 (112 μg m^{-3})		100 (225 μgm^{-3})
SO_2	ppb	30 (80 μg m^{-3})	60 (157 μg m^{-3})		170 (444 μgm^{-3})
H_2S	ppb	6 (8 μg m^{-3})	30 (40 μg m^{-3})		140 (200 μgm^{-3})
CO	ppm		8 (9 mg m^{-3})	10(11.5)	30 (34 mg m^{-3})
O_3	ppb			60 (120)	80 (157 μgm^{-3})
Non-methane Hydrocarbons	ppm				0.24 (3 h mean) 6:00-9:00 am
PM_{10}	μg m^{-3}	90	350		
Mercury	μg m^{-3}	1			

Table 4a: ISCST3 output data modeling results for the 50 highest hourly average concentrations of methane

			Location Coordinate in UTM (m)					Location Coordinate in in UTM (m)	
Rank	CONC. (μg m^{-1})	(YYMMDDHH)	X	Y	Rank	CONC. (μg m^{-1})	(YYMMDDHH)	X	Y
1	2761.5000	6011902	774643.69	3305361.25	26	1159.27	6041903	774643.69	3305361.25
2	2564.3000	6120501	774643.69	3305361.25	27	986.26	6022701	774643.69	3305361.25
3	2464.0000	6040303	774643.69	3305361.25	28	970.53	6041606	774643.69	3305361.25
4	2464.0000	6040601	774643.69	3305361.25	29	954.02	6051002	774643.69	3305361.25
5	2071.1000	6090701	774643.69	3305361.25	30	951.64	6090524	761955.63	3308548.75
6	1898.5000	6042623	774643.69	3305361.25	31	934.89	6041006	774643.69	3305361.25
7	1794.9000	6122607	774643.69	3305361.25	32	915.70	6022407	765127.63	3308548.75
8	1775.2000	6111822	774643.69	3305361.25	33	892.15	6040422	761955.63	3308548.75
9	1725.9000	6021420	774643.69	3305361.25	34	887.63	6060323	774643.69	3305361.25
10	1635.5000	6060705	774643.69	3305361.25	35	886.39	6060101	765127.63	3308548.75
11	1612.8000	6010606	774643.69	3305361.25	36	882.96	6042104	765127.63	3308548.75
12	1612.8000	6011904	774643.69	3305361.25	37	882.96	6042221	765127.63	3308548.75
13	1610.9000	6090224	774643.69	3305361.25	38	855.47	6052805	774643.69	3305361.25
14	1575.3000	6120608	774643.69	3305361.25	39	843.13	6112919	774643.69	3305361.25
15	1557.2000	6091105	765127.63	3308548.75	40	824.89	6062223	774643.69	3305361.25
16	1518.8000	6042124	774643.69	3305361.25	41	805.43	6052505	774643.69	3305361.25
17	1518.8000	6042902	774643.69	3305361.25	42	793.26	6090219	774643.69	3305361.25
18	1475.4000	6090801	774643.69	3305361.25	43	789.01	6100401	774643.69	3305361.25
19	1344.3000	6040504	774643.69	3305361.25	44	784.87	6052604	765127.63	3308548.75
20	1265.7000	6042206	774643.69	3305361.25	45	778.58	6071902	765127.63	3308548.75
21	1264.7000	6060502	774643.69	3305361.25	46	772.87	6042905	774643.69	3305361.25
22	1264.7000	6110503	774643.69	3305361.25	47	743.68	6060524	774643.69	3305361.25
23	1197.7000	6010220	761955.63	3308548.75	48	716.10	6042207	774643.69	3305361.25
24	1191.5000	6120503	774643.69	3305361.25	49	706.91	6022424	765127.63	3308548.75
25	1167.8713	6091922	765127.63	3308548.75	50	702.61	6022720	774643.69	3305361.25

Table 4b: ISCST3 output data modeling results for the 50 highest daily average concentrations of methane

Rank	CONC. (µg m^{-1})	(YYMMDDHH)	Location Coordinate in UTM (m) X	Y	Rank	CONC. (µg m^{-1})	(YYMMDDHH)	Location Coordinate in in UTM (m) X	Y
1	248.49	6011924	774643.69	3305361.25	26	78.346	6090824	774643.69	3305361.25
2	208.66	6120524	774643.69	3305361.25	27	77.105	6100824	774643.69	3305361.25
3	159.85	6042924	774643.69	3305361.25	28	75.908	6091124	765127.63	3308548.75
4	156.94	6040624	774643.69	3305361.25	29	72.511	6040524	774643.69	3305361.25
5	136.89	6040324	774643.69	3305361.25	30	68.994	6091924	765127.63	3308548.75
6	134.01	6090224	774643.69	3305361.25	31	66.552	6010224	761955.63	3308548.75
7	127.98	6022724	774643.69	3305361.25	32	64.040	6010824	774643.69	3305361.25
8	120.64	6060524	774643.69	3305361.25	33	62.837	6113024	774643.69	3305361.25
9	117.64	6090724	774643.69	3305361.25	34	61.357	6120924	765127.63	3308548.75
10	115.44	6042224	774643.69	3305361.25	35	61.036	6041624	774643.69	3305361.25
11	112.14	6122624	774643.69	3305361.25	36	60.766	6060124	765127.63	3308548.75
12	111.75	6022424	765127.63	3308548.75	37	59.883	6012424	774643.69	3305361.25
13	108.44	6012924	765127.63	3308548.75	38	59.298	6022824	774643.69	3305361.25
14	107.91	6100424	774643.69	3305361.25	39	58.420	6012024	774643.69	3305361.25
15	104.91	6010624	774643.69	3305361.25	40	57.395	6101024	774643.69	3305361.25
16	100.32	6080824	774643.69	3305361.25	41	56.456	6092424	774643.69	3305361.25
17	99.11	6111824	774643.69	3305361.25	42	56.160	6122724	774643.69	3305361.25
18	97.57	6042124	774643.69	3305361.25	43	55.527	6012324	765127.63	3308548.75
19	96.88	6110524	774643.69	3305361.25	44	55.392	6102124	774643.69	3305361.25
20	95.36	6042624	774643.69	3305361.25	45	52.766	6041924	774643.69	3305361.25
21	88.78	6021424	774643.69	3305361.25	46	52.696	6041024	774643.69	3305361.25
22	87.53	6120624	774643.69	3305361.25	47	52.469	6041524	774643.69	3305361.25
23	83.76	6060724	774643.69	3305361.25	48	51.177	6100124	774643.69	3305361.25
24	82.24	6041124	774643.69	3305361.25	49	50.572	6112024	774643.69	3305361.25
25	78.83	6062224	774643.69	3305361.25	50	50.545	6101924	774643.69	3305361.25

concentrations of methane, respectively calculated at the uniform grid receptors described previously. Isopleths plots (contours) were generated, as shown in Fig. 8a-c. These present the maximum hourly, daily and annual ground level concentration of methane in µg m^{-3} calculated at the specified uniform grid receptors.

The data presented in Table 4a-c and Fig. 8a-c reveal that predicted ground level concentrations of methane for the specified time exceeds the KAAQS ambient air quality standard over the study area.

As shown in Table 4a the predicted maximum hourly average ground level concentration of methane in the study areas exceeds KAAQS by as much as 2761.5 µg m^{-3}, hour 02:00, 19th January 2006 at the receptor coordinate of X = 774643.69, Y = 3305361.25. As shown in Fig. 8a, this receptor is located nearly 54 km in the NNW direction from the centre of NK Oilfields and not far from the residential areas.

The predicted maximum daily average ground level concentration of methane in the study areas in Table 4b exceeds KAAQS by as much as 248.49 µg m^{-3}, hour 24:00, 19th January 2006 at the receptor coordinate of X = 774643.69, Y = 3305361.25. Inspection of Fig. 8b, this receptor is located nearly 56 km in the NNW

Table 4c: ISCST3 output data modeling results for the 10th highest annual average concentrations of methane

Rank	CONC. (µg m^{-3})	Location Coordinate in UTM (m) X	Y
1ST	6.0005	774643.69	3305361.25
2ND	7.8285	765127.63	3308548.75
3RD	4.5797	761955.63	3311736.00
4TH	3.5772	765127.63	3305361.25
5TH	2.7889	761955.63	3308548.75
6TH	2.4240	768299.69	3302173.75
7TH	2.1309	765127.63	3311736.00
8TH	2.0584	777815.69	3302173.75
9TH	2.0575	768299.69	3305361.25
10TH	1.7195	777815.69	3305361.25

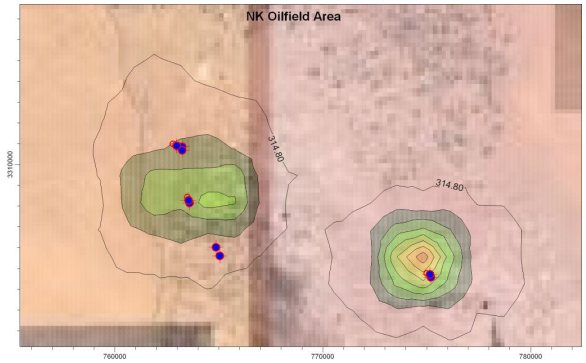

Fig. 8a: Isopleths plot for the maximum hourly average ground level concentrations of methane in µg m^{-3}

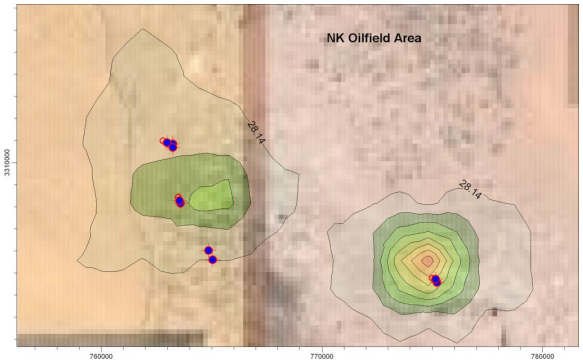

Fig. 8b: Isopleths plot for the maximum hourly average ground level concentrations of methane in μg m^{-3}

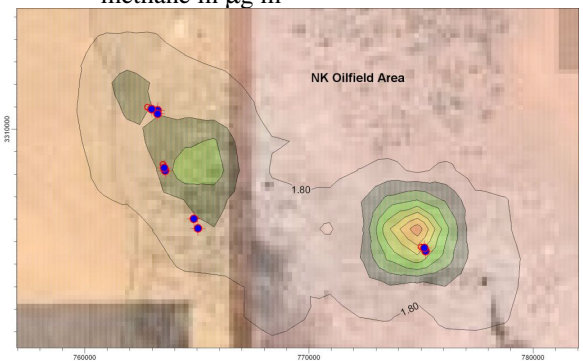

Fig. 8c: Isopleths plot for the maximum annual average ground level concentrations of methane in μg m^{-3}

direction from the centre of NK Oilfields and not far from the residential areas. For the same location, Table 4c and Fig. 8c show that the highest annual maximum concentration of methane is 6 μg m^{-3}.

Non-methane hydrocarbon emissions: Table 5a-c show the modeling results for the 50 highest hourly, 50 highest daily and the 50 highest annual maximum ground level concentrations of non-methane hydrocarbons, respectively calculated at the uniform grid receptors described previously. Isopleths plots (contours) were generated, as shown in Fig. 9a-c. These present the maximum hourly, daily and annual ground level concentration of non-methane hydrocarbons in μg m^{-3} calculated at the specified uniform grid receptors.

The described data reveal that predicted ground level concentrations of non-methane for the specified time exceeds the KAAQS ambient air quality standard over the study area.

As shown in Table 5a and Fig. 9a, the predicted maximum hourly average ground level concentration of non-methane hydrocarbons in the study area exceeds KAAQS by as much as 34442.8 μg m^{-3}, hour 02:00, 19th January 2006 at the a receptor coordinate of X = 774643.69, Y = 3305361.25.

The predicted maximum daily average ground level concentration of non-methane hydrocarbons in the study area given in Table 5b exceeds KAAQS by as much as 3099.8 μg m^{-3}, hour 24:00, 19th January 2006 at the a receptor coordinate of X = 774643.69,

Table 5a: ISCST3 output data modeling results for the 50 highest hourly average concentrations of non-methane hydrocarbons

			Location coordinate in UTM (m)					Location coordinate in UTM (m)	
Rank	CONC. (μg m^{-1})	(YYMMDDHH)	X	Y	Rank	CONC. (μg m^{-1})	(YYMMDDHH)	X	Y
1	34442.8	6011902	774643.69	3305361.25	26	14459.0	6041903	774643.69	3305361.25
2	31983.0	6120501	774643.69	3305361.25	27	13323.0	6090524	761955.63	3308548.75
3	30732.5	6040303	774643.69	3305361.25	28	12819.7	6022407	765127.63	3308548.75
4	30732.5	6040601	774643.69	3305361.25	29	12490.0	6040422	761955.63	3308548.75
5	25831.6	6090701	774643.69	3305361.25	30	12409.5	6060101	765127.63	3308548.75
6	23678.6	6042623	774643.69	3305361.25	31	12361.5	6042104	765127.63	3308548.75
7	22387.5	6122607	774643.69	3305361.25	32	12361.5	6042221	765127.63	3308548.75
8	22141.4	6111822	774643.69	3305361.25	33	12301.2	6022701	774643.69	3305361.25
9	21801.0	6091105	765127.63	3308548.75	34	12105.0	6041606	774643.69	3305361.25
10	21526.0	6021420	774643.69	3305361.25	35	11899.0	6051002	774643.69	3305361.25
11	20398.9	6060705	774643.69	3305361.25	36	11660.4	6041006	774643.69	3305361.25
12	20115.5	6010606	774643.69	3305361.25	37	11071.0	6060323	774643.69	3305361.25
13	20115.5	6011904	774643.69	3305361.25	38	10988.2	6052604	765127.63	3308548.75
14	20091.6	6090224	774643.69	3305361.25	39	10900.1	6071902	765127.63	3308548.75
15	19648.6	6120608	774643.69	3305361.25	40	10669.9	6052805	774643.69	3305361.25
16	18943.3	6042124	774643.69	3305361.25	41	10516.0	6112919	774643.69	3305361.25
17	18943.3	6042902	774643.69	3305361.25	42	10288.5	6062223	774643.69	3305361.25
18	18402.4	6090801	774643.69	3305361.25	43	10045.8	6052505	774643.69	3305361.25
19	16767.7	6010220	761955.63	3308548.75	44	9896.70	6022424	765127.63	3308548.75
20	16767.0	6040504	774643.69	3305361.25	45	9894.00	6090219	774643.69	3305361.25
21	16350.2	6091922	765127.63	3308548.75	46	9840.90	6100401	774643.69	3305361.25
22	15786.3	6042206	774643.69	3305361.25	47	9639.70	6042905	774643.69	3305361.25
23	15774.0	6060502	774643.69	3305361.25	48	9625.20	6011705	765127.63	3308548.75
24	15773.5	6110503	774643.69	3305361.25	49	9306.80	6062923	765127.63	3308548.75
25	14861.2	6120503	774643.69	3305361.25	50	9275.60	6060524	774643.69	3305361.25

Table 5b: ISCST3 output data modeling results for the 50 highest daily average concentrations of non-methane hydrocarbons

Rank	CONC. (μg m^{-1})	(YYMMDDHH)	Location coordinate in UTM (m) X	Y	Rank	CONC. (μg m^{-1})	(YYMMDDHH)	Location coordinate in UTM (m) X	Y
1	3099.8	6011924	774643.69	3305361.3	26	983.20	6062224	774643.69	3305361
2	2602.5	6120524	774643.69	3305361.3	27	978.00	6090824	774643.69	3305361
3	1993.7	6042924	774643.69	3305361.3	28	961.93	6100824	774643.69	3305361
4	1957.5	6040624	774643.69	3305361.3	29	960.11	6091924	765127.63	3308549
5	1707.4	6040324	774643.69	3305361.3	30	931.72	6010224	761955.63	3308549
6	1671.8	6090224	774643.69	3305361.3	31	904.41	6040524	774643.69	3305361
7	1596.2	6022724	774643.69	3305361.3	32	857.01	6120924	765127.63	3308549
8	1564.4	6022424	765127.63	3308548.8	33	850.21	6060124	765127.63	3308549
9	1516.0	6012924	765127.63	3308548.8	34	798.77	6010824	774643.69	3305361
10	1504.6	6060524	774643.69	3305361.3	35	783.73	6113024	774643.69	3305361
11	1469.2	6090724	774643.69	3305361.3	36	773.74	6012324	765127.63	3308549
12	1439.9	6042224	774643.69	3305361.3	37	761.29	6041624	774643.69	3305361
13	1398.7	6122624	774643.69	3305361.3	38	746.89	6012424	774643.69	3305361
14	1346.0	6100424	774643.69	3305361.3	39	739.62	6022824	774643.69	3305361
15	1308.5	6010624	774643.69	3305361.3	40	728.67	6012024	774643.69	3305361
16	1251.3	6080824	774643.69	3305361.3	41	715.86	6101024	774643.69	3305361
17	1236.8	6111824	774643.69	3305361.3	42	704.33	6092424	774643.69	3305361
18	1217.0	6042124	774643.69	3305361.3	43	700.47	6122724	774643.69	3305361
19	1208.3	6110524	774643.69	3305361.3	44	690.88	6102124	774643.69	3305361
20	1190.1	6042624	774643.69	3305361.3	45	661.15	6042224	765127.63	3308549
21	1107.3	6021424	774643.69	3305361.3	46	658.13	6041924	774643.69	3305361
22	1091.7	6120624	774643.69	3305361.3	47	657.26	6041024	774643.69	3305361
23	1059.5	6091124	765127.63	3308548.8	48	654.42	6041524	774643.69	3305361
24	1044.7	6060724	774643.69	3305361.3	49	643.82	6071924	765127.63	3308549
25	1025.7	6041124	774643.69	3305361.3	50	638.44	6100124	774643.69	3305361

Table 5c: ISCST3 output data modeling results for the 10th highest annual average concentrations of non-methane hydrocarbons

Rank	CONC. (μg m^{-3})	Location Coordinate in UTM (m) X	Y
1ST	200.17	774643.69	3305361.25
2ND	107.89	765127.63	3308548.75
3RD	63.14	761955.63	3311736.00
4TH	49.68	765127.63	3305361.25
5TH	38.77	761955.63	3308548.75
6TH	33.04	768299.69	3302173.75
7TH	29.04	765127.63	3311736.00
8TH	27.98	768299.69	3305361.25
9TH	26.21	777815.69	3302173.75
10TH	22.79	768299.69	3308548.75

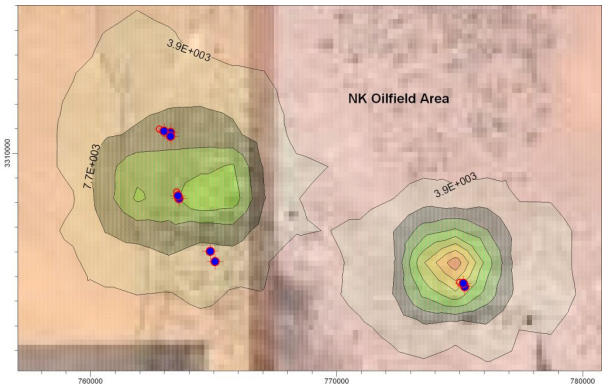

Fig. 9a: Isopleths plot for the maximum hourly average ground level concentrations of non-methane hydrocarbons in μg m^{-3}

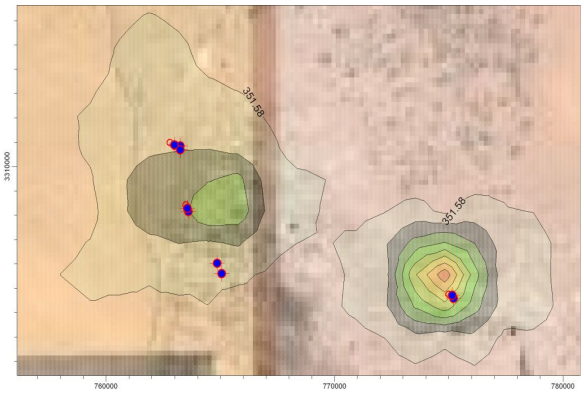

Fig. 9b: Isopleths plot for the maximum hourly average ground level concentrations of non-methane hydrocarbons in μg m^{-3}

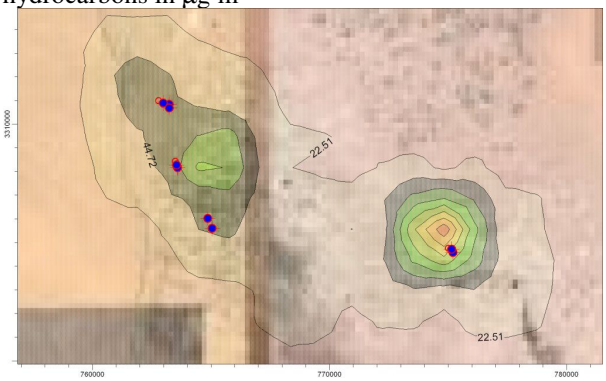

Fig. 9c: Isopleths plot for the maximum annual average ground level concentrations of non-methane hydrocarbons in μg m^{-3}

Y = 3305361.25. This receptor is located nearly 54 km in the NNW direction from the centre of the NK Oilfields and not far from the residential areas. For the same location, Table 5c and Fig. 9c show that the highest annual maximum concentration of non-methane hydrocarbons is 200.17 μg m^{-3}.

There were some unexpected problems in NK Oilfields in the year 2005 and the amount of gas flared, as a percentage of production, was almost double of the amount recorded from 2004. The above results reflect this, as well as, the increase in flaring in January 2006, due to regular shut down of Condensate Recovery Unit (CRU's) in NK Oilfields and the prevailing wind direction in Kuwait. Considering Table 4a-c, 5a-c and Fig. 8a-c, 9a-c together, it can be concluded the weather pattern in Kuwait in January 2006, especially the mean prevailing wind direction, significantly contributed to high concentrations of methane and non-methane hydrocarbons at ground level in residential areas located downwind of the NK Oilfields.

South and East Kuwait oilfield area results

Non-methane hydrocarbons emission: Table 6a-c show the modeling results for the 50 highest hourly, 50 highest daily and the 50 highest annual maximum ground level concentrations of non-methane hydrocarbons, respectively calculated at the uniform grid receptors described previously. Isopleths plots (contours) were generated, as show in Fig. 10a-c. These present the maximum hourly, daily and annual ground level concentration of non-methane hydrocarbons in μg m^{-3} calculated at the specified uniform grid receptors.

As shown in Table 6a the predicted maximum hourly average ground level concentration of non-methane hydrocarbons in the study area is 5363 μg m^{-3}, hour 2:00, 28th January 2006 at the receptor coordinate of X = 790158.13, Y = 3203288.25

The predicted maximum daily average ground level concentration of non-methane hydrocarbons in the study area in Table 6b is 473.15 μg m^{-3}, hour 24:00, 16th January 2006 at the receptor coordinate of X = 790158.13, Y = 3203288.25. For the same location, Table 6c and Fig. 10c show that the highest annual maximum concentration of non-methane hydrocarbons is 17.943 μg m^{-3}.

Methane emission: Table 7a-c show the modeling results for the 50 highest hourly, 50 highest daily and the 50 highest annual maximum ground level concentrations of methane, respectively calculated at the uniform grid

Fig. 10a: Isopleths plot for the maximum hourly average ground level concentrations of non-methane hydrocarbons in μg-m^3

Fig. 10b: Isopleths plot for the maximum hourly average ground level concentrations of non-methane hydrocarbons in μg m^{-3}

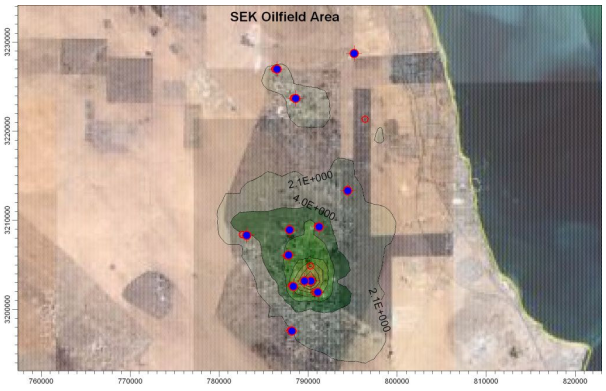

Fig. 10c: Isopleths plot for the maximum annual average ground level concentrations of non-methane hydrocarbons in μg m^{-3}

Table 6a: ISCST3 output data modeling results for the 50 highest hourly average concentrations of non-methane hydrocarbons

Rank	CONC. (μg m^{-1})	(YYMMDDHH)	Location coordinate in UTM (m) X	Y	Rank	CONC. (μg m^{-1})	(YYMMDDHH)	Location coordinate in UTM (m) X	Y
1	5363.0	6012802	790158.13	3203288.25	26	1125.3	6052023	790158.13	3209777.50
2	4841.0	6011605	790158.13	3203288.25	27	1089.7	6122319	786283.06	3206532.75
3	4501.3	6011609	790158.13	3203288.25	28	1034.8	6062302	782408.00	3209777.50
4	3824.7	6010222	790158.13	3203288.25	29	1032.7	6062221	782408.00	3209777.50
5	3118.6	6011306	790158.13	3203288.25	30	1027.8	6022320	790158.13	3203288.25
6	2270.7	6012803	790158.13	3203288.25	31	984.00	6022222	790158.13	3203288.25
7	2093.5	6060222	782408.00	3209777.50	32	967.90	6052804	790158.13	3206532.75
8	1962.3	6081904	786283.06	3206532.75	33	917.70	6060202	782408.00	3209777.50
9	1913.8	6052023	790158.13	3206532.75	34	897.00	6051422	790158.13	3203288.25
10	1880.7	6052802	790158.13	3206532.75	35	888.30	6050202	794033.19	3206532.75
11	1869.8	6062305	782408.00	3209777.50	36	888.30	6051503	794033.19	3206532.75
12	1793.4	6060306	790158.13	3203288.25	37	860.60	6060522	782408.00	3209777.50
13	1702.9	6012308	790158.13	3203288.25	38	857.10	6120621	786283.06	3226000.50
14	1674.8	6060201	782408.00	3209777.50	39	856.50	6022507	790158.13	3203288.25
15	1674.8	6060723	782408.00	3209777.50	40	851.30	6052005	790158.13	3203288.25
16	1616.0	6011421	790158.13	3203288.25	41	838.60	6120504	786283.06	3209777.50
17	1563.6	6060403	790158.13	3203288.25	42	819.60	6122801	786283.06	3209777.50
18	1473.6	6011422	790158.13	3203288.25	43	815.50	6081303	786283.06	3206532.75
19	1345.5	6050324	790158.13	3203288.25	44	797.40	6051119	790158.13	3203288.25
20	1343.9	6050904	790158.13	3206532.75	45	790.70	6050921	790158.13	3206532.75
21	1323.5	6060301	790158.13	3203288.25	46	781.80	6051624	786283.06	3209777.50
22	1323.5	6062806	790158.13	3203288.25	47	781.80	6051724	786283.06	3209777.50
23	1260.9	6120201	790158.13	3209777.50	48	767.70	6050820	790158.13	3209777.50
24	1166.8	6062301	790158.13	3206532.75	49	765.40	6050720	786283.06	3200043.50
25	1137.6	6122522	790158.13	3209777.50	50	764.10	6081923	790158.13	3209777.50

Table 6b: ISCST3 output data modeling results for the 50 highest daily average concentrations of non-methane hydrocarbons

Rank	CONC. (μg m^{-1})	in UTM (m) (YYMMDDHH)	Location coordinate X	Y	Rank	CONC. (μg m^{-1})	in UTM (m) (YYMMDDHH)	Location coordinate in X	Y
1	473.15	6011624	790158.13	3203288.25	26	68.452	6051124	790158.13	3203288.25
2	437.21	6012824	790158.13	3203288.25	27	67.492	6090224	790158.13	3203288.25
3	300.76	6060224	782408.00	3209777.5	28	67.388	6080724	790158.13	3203288.25
4	221.51	6010224	790158.13	3203288.25	29	67.377	6120224	790158.13	3209777.50
5	173.01	6060324	790158.13	3203288.25	30	66.431	6050224	790158.13	3203288.25
6	170.67	6011324	790158.13	3203288.25	31	66.254	6060524	782408.00	3209777.50
7	164.52	6062324	782408.00	3209777.5	32	65.009	6062824	790158.13	3203288.25
8	149.51	6011424	790158.13	3203288.25	33	63.242	6050724	786283.06	3200043.50
9	136.67	6081924	786283.06	3206532.75	34	62.776	6122324	786283.06	3206532.75
10	128.76	6052824	790158.13	3206532.75	35	62.759	6081924	790158.13	3209777.50
11	124.52	6050924	790158.13	3206532.75	36	62.325	6120924	790158.13	3203288.25
12	107.87	6073124	790158.13	3203288.25	37	61.972	6122624	786283.06	3209777.50
13	103.05	6012324	790158.13	3203288.25	38	61.421	6121224	790158.13	3203288.25
14	102.61	6060424	790158.13	3203288.25	39	60.210	6060224	794033.19	3216266.50
15	92.28	6060724	782408.00	3209777.5	40	59.873	6062224	782408.00	3209777.50
16	90.41	6042124	790158.13	3203288.25	41	58.442	6021524	790158.13	3196799.00
17	90.30	6062324	790158.13	3206532.75	42	58.091	6032424	790158.13	3203288.25
18	86.85	6022524	790158.13	3203288.25	43	57.849	6042024	790158.13	3203288.25
19	86.25	6022224	790158.13	3203288.25	44	57.177	6122524	790158.13	3209777.50
20	83.06	6052024	790158.13	3206532.75	45	57.159	6051724	786283.06	3209777.50
21	82.22	6120224	790158.13	3203288.25	46	56.912	6030324	790158.13	3203288.25
22	82.02	6051424	790158.13	3203288.25	47	56.626	6010124	790158.13	3203288.25
23	81.04	6022324	790158.13	3203288.25	48	56.570	6082324	790158.13	3206532.75
24	80.41	6052024	790158.13	3209777.5	49	55.211	6052024	790158.13	3203288.25
25	76.19	6050324	790158.13	3203288.25	50	54.337	6120524	794033.19	3213022.00

receptors described previously. Isopleths plots (contours) were generated, as shown in Fig. 11a-c. These present the maximum hourly, daily and annual ground level concentration of methane in μg m^{-3} calculated at the specified uniform grid receptors.

Fig. 11a: Isopleths plot for the maximum hourly average ground level concentrations of methane in µg m^{-3}

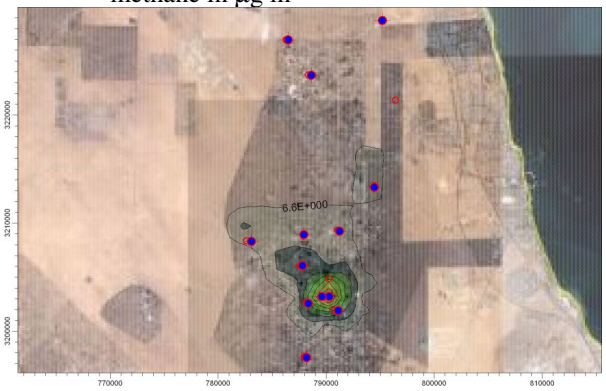

Fig. 11b: Isopleths plot for the maximum hourly average ground level concentrations of methane in µg m^{-3}

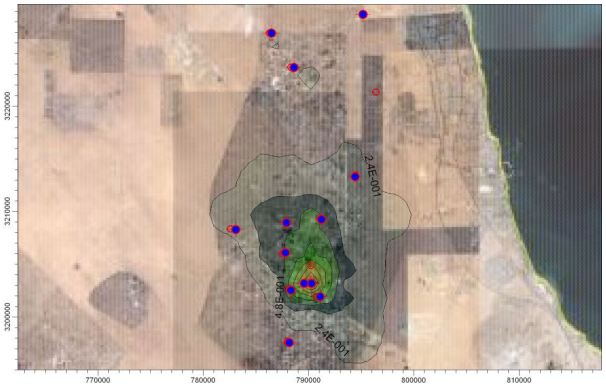

Fig. 11c: Isopleths plot for the maximum annual average ground level concentrations of methane in µg m^{-3}

Table 6c: ISCST3 output data modeling results for the 10th highest annual average concentrations of non-methane hydrocarbons

Rank	CONC. (µg m^{-3})	Location Coordinate in UTM (m) X	Y
1ST	17.943	790158.13	3203288.25
2ND	7.664	790158.13	3206532.75
3RD	6.447	790158.13	3209777.50
4TH	5.869	782408.00	3209777.50
5TH	5.429	786283.06	3206532.75
6TH	5.133	786283.06	3209777.50
7TH	4.082	794033.19	3200043.50
8TH	4.014	790158.13	3200043.50
9TH	3.960	790158.13	3222755.75
10TH	3.776	786283.06	3203288.25

Table 7a: ISCST3 output data modeling results for the 50 highest hourly average concentrations of methane

Rank	CONC. (µg m^{-1})	(YYMMDDHH)	Location coordinate in UTM (m) X	Y	Rank	CONC. (µg m^{-1})	(YYMMDDHH)	Location coordinate in UTM (m) X	Y
1	655.48	6012802	790158.13	3203288.25	26	114.04	6122623	786283.06	3209777.50
2	591.66	6011605	790158.13	3203288.25	27	104.77	6121324	790158.13	3206532.75
3	550.10	6011609	790158.13	3203288.25	28	104.69	6022507	790158.13	3203288.25
4	467.41	6010222	790158.13	3203288.25	29	102.08	6050324	790158.13	3203288.25
5	381.15	6011306	790158.13	3203288.25	30	101.12	6050904	790158.13	3206532.75
6	277.53	6012803	790158.13	3203288.25	31	98.520	6060222	782408.00	3209777.50
7	240.39	6081904	786283.06	3206532.75	32	96.940	6081303	786283.06	3206532.75
8	219.01	6060306	790158.13	3203288.25	33	93.740	6120522	794033.19	3213022.00
9	208.14	6012308	790158.13	3203288.25	34	93.060	6120222	790158.13	3203288.25
10	197.38	6011421	790158.13	3203288.25	35	92.010	6120904	790158.13	3203288.25
11	196.69	6120201	790158.13	3209777.50	36	89.580	6062301	790158.13	3206532.75
12	190.99	6060403	790158.13	3203288.25	37	88.970	6121202	790158.13	3209777.50
13	178.14	6011422	790158.13	3203288.25	38	87.990	6062305	782408.00	3209777.50
14	177.47	6122522	790158.13	3209777.50	39	86.440	6012110	790158.13	3203288.25
15	168.72	6122319	786283.06	3206532.75	40	85.980	6031302	790158.13	3206532.75
16	161.77	6060301	790158.13	3203288.25	41	85.380	6100807	782408.00	3209777.50
17	161.77	6062806	790158.13	3203288.25	42	84.750	6052023	790158.13	3209777.50
18	143.59	6052023	790158.13	3206532.75	43	84.580	6120221	790158.13	3203288.25
19	141.62	6052802	790158.13	3206532.75	44	84.330	6082107	790158.13	3203288.25
20	130.82	6120504	786283.06	3209777.50	45	83.060	6050820	790158.13	3209777.50
21	127.85	6122801	786283.06	3209777.50	46	82.890	6120621	786283.06	3226000.50
22	125.62	6022320	790158.13	3203288.25	47	82.660	6081923	790158.13	3209777.50
23	120.27	6022222	790158.13	3203288.25	48	80.650	6010222	790158.13	3209777.50
24	118.10	6121919	790158.13	3209777.50	49	80.570	6022504	790158.13	3203288.25
25	118.05	6060403	790158.13	3209777.50	50	78.820	6060201	782408.00	3209777.50

Table 7b: ISCST3 output data modeling results for the 50 highest daily average concentrations of methane

Rank	CONC. ($\mu g\ m^{-1}$)	(YYMMDDHH)	Location coordinate in UTM (m) X	Y	Rank	CONC. ($\mu g\ m^{-1}$)	(YYMMDDHH)	Location coordinate in UTM (m) X	Y
1	57.647	6011624	790158.13	3203288.25	26	8.0623	6121224	790158.13	3209777.50
2	53.834	6012824	790158.13	3203288.25	27	8.0610	6060424	790158.13	3209777.50
3	27.317	6010224	790158.13	3203288.25	28	7.8103	6062324	782408.00	3209777.50
4	21.604	6060324	790158.13	3203288.25	29	7.7851	6051424	790158.13	3203288.25
5	20.799	6011324	790158.13	3203288.25	30	7.5105	6120924	790158.13	3203288.25
6	17.948	6011424	790158.13	3203288.25	31	7.4939	6120524	786283.06	3209777.50
7	16.712	6081924	786283.06	3206532.75	32	7.3881	6062324	790158.13	3206532.75
8	14.424	6060224	782408.00	3209777.50	33	7.3228	6062824	790158.13	3203288.25
9	13.023	6073124	790158.13	3203288.25	34	7.1998	6030324	790158.13	3203288.25
10	12.645	6012324	790158.13	3203288.25	35	7.1559	6052024	790158.13	3209777.50
11	12.023	6060424	790158.13	3203288.25	36	7.1476	6042024	790158.13	3203288.25
12	11.127	6042124	790158.13	3203288.25	37	7.1346	6121224	790158.13	3203288.25
13	10.554	6022524	790158.13	3203288.25	38	6.9845	6080724	790158.13	3203288.25
14	10.321	6022224	790158.13	3203288.25	39	6.6626	6032424	790158.13	3203288.25
15	10.128	6052824	790158.13	3206532.75	40	6.5900	6082724	786283.06	3209777.50
16	9.988	6120224	790158.13	3209777.50	41	6.5720	6081924	790158.13	3209777.50
17	9.963	6120224	790158.13	3203288.25	42	6.4544	6082124	790158.13	3203288.25
18	9.569	6122324	786283.06	3206532.75	43	6.3392	6052024	790158.13	3206532.75
19	9.541	6022324	790158.13	3203288.25	44	6.3372	6121924	790158.13	3209777.50
20	9.505	6122624	786283.06	3209777.50	45	6.1642	6012924	790158.13	3203288.25
21	9.460	6050924	790158.13	3206532.75	46	5.8714	6121324	790158.13	3206532.75
22	9.194	6060224	794033.19	3216266.50	47	5.8424	6050324	790158.13	3203288.25
23	8.894	6122524	790158.13	3209777.50	48	5.7982	6050224	790158.13	3203288.25
24	8.640	6090224	790158.13	3203288.25	49	5.6505	6010224	790158.13	3209777.50
25	8.27222	6120524	794033.19	3213022.00	50	5.6304	6081324	786283.06	3206532.75

Table 7c: ISCST3 output data modeling results for the 10th highest annual average concentrations of methane

Rank	CONC. ($\mu g\ m^{-3}$)	Location coordinate in UTM (m) X	Y
1ST	2.1248	790158.13	3203288.25
2ND	0.9741	790158.13	3206532.75
3RD	0.8148	790158.13	3209777.50
4TH	0.6234	786283.06	3209777.50
5TH	0.5387	786283.06	3206532.75
6TH	0.4309	794033.19	3200043.50
7TH	0.4194	782408.00	3209777.50
8TH	0.3830	794033.19	3203288.25
9TH	0.3763	794033.19	3206532.75
10TH	0.3579	786283.06	3213022.00

As shown in Table 7a the predicted maximum hourly average ground level concentration of methane in the study area is 655.48 $\mu g\ m^{-3}$, hour 2:00, 28th January 2006 at the receptor coordinate of X = 790158.13, Y = 3203288.25.

The predicted maximum daily average ground level concentration of methane in the study area in Table 7b is 57.647 $\mu g\ m^{-3}$, hour 24:00, 16th January 2006 at the a receptor coordinate of X = 790158.13, Y = 3203288.25. For the same location, Table 7c and Fig. 11c show that the highest annual maximum concentration of methane is 2.125 $\mu g\ m^{-3}$.

The main reasons for high levels of methane and non-methane hydrocarbons encountered in the above results is the increased amount of flaring in January 2006 resulting from frequent shutdowns of CRU's, shortage of gas compression facilities and malfunction of the BS's in SEK Oilfields. Again, these data given strong indication regarding the significant influence prevailing wind direction on the ground level concentrations of methane and non-methane hydrocarbons.

West Kuwait oilfield area results

Non-methane hydrocarbons emission: Table 8a-c show the modeling results for the 50 highest hourly, 50 highest daily and the 50 highest annual maximum ground level concentrations of non-methane hydrocarbons, respectively calculated at the uniform grid receptors described previously. Isopleths plots (contours) were generated, as show in Fig. 12a-c. These present the maximum hourly, daily and annual ground level concentration of non-methane hydrocarbons in $\mu g\ m^{-3}$ calculated at the specified uniform grid receptors.

As shown in Table 8a the predicted maximum hourly average ground level concentration of non-methane hydrocarbons in the study area is 3485.2 $\mu g\ m^{-3}$, hour 15:00, 25th August 2006 at the receptor coordinate of X = 766258.06, Y = 3192914.25.

The predicted maximum daily average ground level concentration of non-methane hydrocarbons in

Table 8a: ISCST3 output data modeling results for the 50 highest hourly average concentrations of non-methane hydrocarbons

			Location coordinate in UTM (m)					Location coordinate in UTM (m)	
Rank	CONC. ($\mu g\ m^{-1}$)	(YYMMDDHH)	X	Y	Rank	CONC. ($\mu g\ m^{-1}$)	(YYMMDDHH)	X	Y
1	3485.2	6082515	766258.06	3192914.25	26	1813.7	6081119	758013.31	3195557.75
2	3368.0	6082010	766258.06	3192914.25	27	1788.7	6081611	766258.06	3192914.25
3	3354.5	6082508	766258.06	3192914.25	28	1778.0	6082509	766258.06	3192914.25
4	3077.2	6080710	766258.06	3192914.25	29	1776.4	6082207	769006.31	3192914.25
5	2679.4	6082810	766258.06	3192914.25	30	1771.2	6102715	766258.06	3192914.25
6	2400.9	6081308	766258.06	3192914.25	31	1748.3	6081119	755265.13	3195557.75
7	2395.5	6080609	766258.06	3192914.25	32	1741.6	6082212	766258.06	3192914.25
8	2374.9	6080812	766258.06	3192914.25	33	1705.8	6092209	766258.06	3192914.25
9	2204.5	6090209	766258.06	3192914.25	34	1698.9	6082812	749768.63	3214061.00
10	2155.3	6080207	771754.56	3198201.00	35	1679.9	6092612	766258.06	3192914.25
11	2129.5	6081517	763509.81	3192914.25	36	1672.5	6082612	749768.63	3214061.00
12	2124.0	6071313	766258.06	3192914.25	37	1672.1	6082811	749768.63	3214061.00
13	2079.1	6080617	766258.06	3192914.25	38	1621.8	6081018	760761.56	3192914.25
14	2057.2	6082414	766258.06	3192914.25	39	1619.8	6101111	766258.06	3192914.25
15	2051.2	6090710	766258.06	3195557.75	40	1607.2	6073116	766258.06	3192914.25
16	2029.1	6082112	766258.06	3192914.25	41	1601.2	6082410	766258.06	3192914.25
17	1994.3	6082516	763509.81	3195557.75	42	1600.1	6080507	769006.31	3195557.75
18	1981.6	6070407	771754.56	3195557.75	43	1588.8	6070415	766258.06	3192914.25
19	1916.9	6072212	766258.06	3192914.25	44	1587.0	6081115	766258.06	3192914.25
20	1847.2	6082416	766258.06	3192914.25	45	1583.0	6081211	766258.06	3192914.25
21	1841.2	6080814	766258.06	3192914.25	46	1576.1	6081408	769006.31	3190271.00
22	1838.6	6082808	769006.31	3195557.75	47	1542.6	6070407	774502.75	3195557.75
23	1832.1	6073108	769006.31	3195557.75	48	1523.7	6072612	766258.06	3192914.25
24	1821.4	6081006	769006.31	3192914.25	49	1505.0	6091717	766258.06	3192914.25
25	1814.3	6081118	763509.81	3192914.25	50	1488.5	6070312	766258.06	3192914.25

Table 8b: ISCST3 output data modeling results for the 50 highest daily average concentrations of non-methane hydrocarbons

			Location coordinate in UTM (m)					Location coordinate in UTM (m)	
Rank	CONC. ($\mu g\ m^{-1}$)	(YYMMDDHH)	X	Y	Rank	CONC. ($\mu g\ m^{-1}$)	(YYMMDDHH)	X	Y
1	492.17	6082524	766258.06	3192914.25	26	198.25	6091724	766258.06	3190271.00
2	467.97	6082424	766258.06	3192914.25	27	197.94	6090724	766258.06	3195557.75
3	360.05	6080324	769006.31	3190271.00	28	197.87	6072624	771754.56	3184984.25
4	355.36	6070824	769006.31	3190271.00	29	197.59	6081124	766258.06	3192914.25
5	328.49	6080624	766258.06	3192914.25	30	195.32	6072824	771754.56	3187627.50
6	302.04	6080324	771754.56	3187627.50	31	193.49	6070724	769006.31	3190271.00
7	295.17	6072024	769006.31	3190271.00	32	191.29	6072224	766258.06	3192914.25
8	288.18	6092224	766258.06	3192914.25	33	189.96	6080824	766258.06	3192914.25
9	274.19	6072724	771754.56	3187627.50	34	189.02	6080124	769006.31	3190271.00
10	267.53	6091724	766258.06	3192914.25	35	188.85	6082024	766258.06	3192914.25
11	262.78	6071224	769006.31	3192914.25	36	187.99	6050724	766258.06	3192914.25
12	255.87	6080524	769006.31	3190271.00	37	186.24	6090424	769006.31	3190271.00
13	255.65	6072724	769006.31	3190271.00	38	186.20	6080324	752516.88	3211417.75
14	246.50	6071624	769006.31	3190271.00	39	186.06	6092324	766258.06	3192914.25
15	241.79	6072624	766258.06	3192914.25	40	183.57	6080524	771754.56	3187627.50
16	239.11	6071824	769006.31	3190271.00	41	183.46	6073124	769006.31	3195557.75
17	233.31	6072824	769006.31	3190271.00	42	182.48	6072024	771754.56	3190271.00
18	229.73	6082824	749768.63	3214061.00	43	182.15	6071924	766258.06	3192914.25
19	216.64	6072724	774502.75	3184984.25	44	181.75	6070924	769006.31	3190271.00
20	214.42	6071024	771754.56	3190271.00	45	181.74	6091024	766258.06	3192914.25
21	208.90	6082824	766258.06	3192914.25	46	181.57	6070824	771754.56	3187627.50
22	206.61	6080324	774502.75	3184984.25	47	180.85	6081024	769006.31	3192914.25
23	205.34	6080224	769006.31	3190271.00	48	176.36	6071124	769006.31	3192914.25
24	201.87	6090124	766258.06	3192914.25	49	176.10	6082424	766258.06	3190271.00
25	200.32	6071924	769006.31	3187627.50	50	175.83	6081224	766258.06	3192914.25

the study area in Table 8b is 492.17 $\mu g\ m^{-3}$, hour 24:00, 28th August 2006 at the receptor coordinate of X = 766258.06, Y = 3192914.25. For the same location, Table 8b and Fig. 12c show that the highest annual maximum concentration of non-methane hydrocarbons is 45.639 $\mu g\ m^{-3}$.

Table 8c: ISCST3 output data modeling results for the 10th highest annual average concentrations of non-methane hydrocarbons

Rank	CONC. (µg m^{-3})	Location coordinate in UTM (m) X	Y
1ST	45.639	766258.06	3192914.25
2ND	44.757	769006.31	3190271.00
3RD	31.182	771754.56	3187627.50
4TH	29.452	769006.31	3192914.25
5TH	27.076	771754.56	3190271.00
6TH	23.262	769006.31	3195557.75
7TH	23.102	755265.13	3208774.25
8TH	22.776	774502.75	3184984.25
9TH	21.799	752516.88	3211417.75
10TH	21.220	771754.56	3184984.25

Fig. 12a: Isopleths plot for the maximum hourly average ground level concentrations of non-methane hydrocarbons in µg m^{-3}

Methane emission: Table 9a-c show the modeling results for the 50 highest hourly, 50 highest daily and the 50 highest annual maximum ground level concentrations of methane, respectively calculated at the uniform grid receptors described previously. Isopleths plots (contours) were generated, as show in Fig. 13a-13c. These present the maximum hourly, daily and annual ground level concentration of methane in µg m^{-3} calculated at the specified uniform grid receptors.

As shown in Table 9a the predicted maximum hourly average ground level concentration of methane in the study area is 221.02 µg m^{-3}, hour 15:00, 25th August 2006 at the receptor coordinate of X = 766258.06, Y = 3192914.25.

The predicted maximum daily average ground level concentration of methane in the study area in Table 9b is 31.075 µg m^{-3}, hour 24:00, 25th August 2006 at the receptor coordinate of X = 766258.06, Y = 3192914.25. For the same location, Table 9c and Fig. 13c show that the highest annual maximum concentration of methane is 2.764 µg m^{-1}.

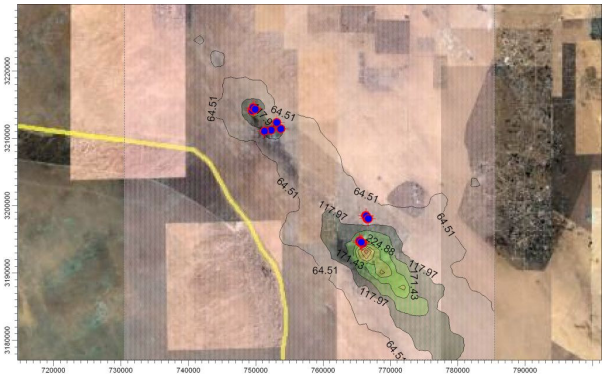

Fig. 12b: Isopleths plot for the maximum hourly average ground level concentrations of non-methane hydrocarbons in µg m^{-3}

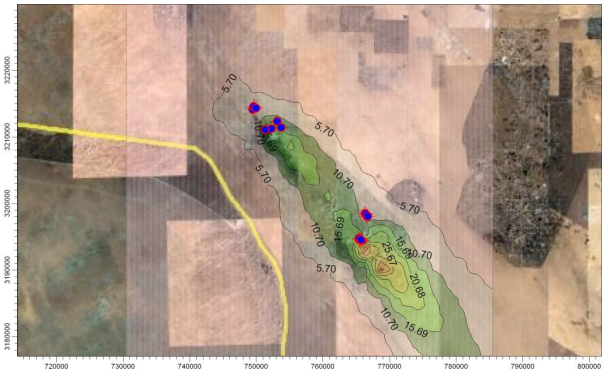

Fig. 12c: Isopleths plot for the maximum annual average ground level concentrations of non-methane hydrocarbons in µg m^{-3}

The above data reflect the increase of emissions as a result of increase in flaring in August 2006 due to regular shut down of Shuaiba AGRP and CRU's of WK gathering centers. In addition to this complete shutdown of the two main GC's in WK Oilfields for survey, have contributed to the increase of flaring.

After the comparison between the simulated results for emission scenarios in the North, Southeast and West Kuwait Oilfields it can be concluded the following:

- NK Oilfields have generated a high ground level concentration of methane and non-methane hydrocarbons emissions than SEK and WK Oilfields. This is because of the unexpected problems in NK Oilfields. The amount of gas flared in these fluids as a percentage of production in January 2006, was about double that of the previous year

Table 9a: ISCST3 output data modeling results for the 50 highest hourly average concentrations of methane

Rank	CONC. ($\mu g\ m^{-1}$)	(YYMMDDHH)	Location coordinate in UTM (m) X	Y	Rank	CONC. ($\mu g\ m^{-1}$)	(YYMMDDHH)	Location coordinate in UTM (m) X	Y
1	221.02	6082515	766258.06	3192914.25	26	113.77	06082509)	766258.06	3192914.25
2	215.04	6082010	766258.06	3192914.25	27	112.97	06081611)	766258.06	3192914.25
3	210.59	6082508	766258.06	3192914.25	28	112.08	06102715)	766258.06	3192914.25
4	196.66	6080710	766258.06	3192914.25	29	111.79	06082808)	769006.31	3195557.75
5	168.83	6082810	766258.06	3192914.25	30	111.38	06081119)	758013.31	3195557.75
6	151.52	6080609	766258.06	3192914.25	31	111.30	06081006)	769006.31	3192914.25
7	150.89	6080812	766258.06	3192914.25	32	108.72	06081119)	755265.13	3195557.75
8	140.86	6081308	766258.06	3192914.25	33	108.65	06081118)	763509.81	3192914.25
9	138.19	6090209	766258.06	3192914.25	34	108.20	06082111)	749768.63	3214061.00
10	134.56	6080207	771754.56	3198201.00	35	108.01	06082212)	766258.06	3192914.25
11	134.38	6081517	763509.81	3192914.25	36	107.10	06092209)	766258.06	3192914.25
12	134.31	6071313	766258.06	3192914.25	37	106.43	06082207)	769006.31	3192914.25
13	133.99	6082812	749768.63	3214061.00	38	105.47	06092612)	766258.06	3192914.25
14	131.91	6082612	749768.63	3214061.00	39	103.23	06101111)	766258.06	3192914.25
15	131.88	6082811	749768.63	3214061.00	40	101.37	06081018)	760761.56	3192914.25
16	131.30	6080617	766258.06	3192914.25	41	101.35	06073116)	766258.06	3192914.25
17	130.63	6082414	766258.06	3192914.25	42	99.80	06070415)	766258.06	3192914.25
18	128.14	6082112	766258.06	3192914.25	43	99.44	06081408)	769006.31	3190271.00
19	126.85	6090710	766258.06	3195557.75	44	99.34	06082410)	766258.06	3192914.25
20	123.48	6082516	763509.81	3195557.75	45	98.97	06080507)	769006.31	3195557.75
21	122.33	6072212	766258.06	3192914.25	46	98.59	06081211)	766258.06	3192914.25
22	121.57	6070407	771754.56	3195557.75	47	96.99	06081115)	766258.06	3192914.25
23	117.76	6082416	766258.06	3192914.25	48	96.73	06070407)	774502.75	3195557.75
24	116.84	6080814	766258.06	3192914.25	49	96.68	06072612)	766258.06	3192914.25
25	116.02	6073108	769006.31	3195557.75	50	94.90	06091717)	766258.06	3192914.25

Table 9b: ISCST3 output data modeling results for the 50 highest daily average concentrations of methane

Rank	CONC. ($\mu g\ m^{-1}$)	(YYMMDDHH)	Location coordinate in UTM (m) X	Y	Rank	CONC. ($\mu g\ m^{-1}$)	(YYMMDDHH)	Location coordinate in UTM (m) X	Y
1	31.074	6082524	766258.06	3192914.25	26	12.561	6071924	769006.31	3187627.50
2	29.548	6082424	766258.06	3192914.25	27	12.552	6072624	771754.56	3184984.25
3	22.549	6080324	769006.31	3190271.00	28	12.457	6090124	766258.06	3192914.25
4	22.408	6070824	769006.31	3190271.00	29	12.447	6091724	766258.06	3190271.00
5	20.503	6080624	766258.06	3192914.25	30	12.443	6072824	771754.56	3187627.50
6	19.284	6080324	771754.56	3187627.50	31	12.393	6081124	766258.06	3192914.25
7	18.542	6072024	769006.31	3190271.00	32	12.103	6070724	769006.31	3190271.00
8	18.127	6082824	749768.63	3214061.00	33	12.100	6072224	766258.06	3192914.25
9	18.126	6092224	766258.06	3192914.25	34	12.053	6082024	766258.06	3192914.25
10	17.270	6072724	771754.56	3187627.50	35	11.968	6080824	766258.06	3192914.25
11	16.927	6091724	766258.06	3192914.25	36	11.896	6080124	769006.31	3190271.00
12	16.142	6071224	769006.31	3192914.25	37	11.832	6090724	766258.06	3195557.75
13	16.104	6080524	769006.31	3190271.00	38	11.818	6090424	769006.31	3190271.00
14	15.844	6072724	769006.31	3190271.00	39	11.783	6080524	771754.56	3187627.50
15	15.535	6071624	769006.31	3190271.00	40	11.728	6072024	771754.56	3190271.00
16	15.143	6071824	769006.31	3190271.00	41	11.685	6070824	771754.56	3187627.50
17	15.076	6072624	766258.06	3192914.25	42	11.504	6092324	766258.06	3192914.25
18	14.686	6080324	752516.88	3211417.75	43	11.388	6070924	769006.31	3190271.00
19	14.553	6072824	769006.31	3190271.00	44	11.371	6081024	769006.31	3192914.25
20	13.805	6072724	774502.75	3184984.25	45	11.369	6050724	766258.06	3192914.25
21	13.401	6080324	774502.75	3184984.25	46	11.340	6073124	769006.31	3195557.75
22	13.384	6071024	771754.56	3190271.00	47	11.209	6082424	766258.06	3190271.00
23	13.257	6082824	766258.06	3192914.25	48	11.087	6080424	769006.31	3190271.00
24	13.246	6082524	749768.63	3214061.00	49	11.065	6081224	766258.06	3192914.25
25	12.973	6080224	769006.31	3190271.00	50	11.050	6072724	777251.00	3182341.00

- Methane and non-methane hydrocarbons are not the only green house gasses which result from flaring activities. The flaring of excess gas is the largest single source of atmospheric emissions arising from KOC operations. However, flaring produces carbon dioxide, oxides of sulphur and nitrogen (NOx) and other chemical species that are produced due to incomplete combustion, such as carbon monoxide, aldehydes, ketones and other organic compounds known as VOCs (Volatile

Table 9c: ISCST3 output data modeling results for the 10th highest annual average concentrations of methane

Rank	CONC. (µg m^{-3})	Location coordinate in UTM (m) X	Y
1ST	2.7643	766258.06	3192914.25
2ND	2.7639	769006.31	3190271.00
3RD	1.9585	771754.56	3187627.50
4TH	1.8554	769006.31	3192914.25
5TH	1.7187	771754.56	3190271.00
6TH	1.6407	755265.13	3208774.25
7TH	1.5455	752516.88	3211417.75
8TH	1.5096	769006.31	3195557.75
9TH	1.4454	774502.75	3184984.25
10TH	1.3404	758013.31	3206131.00

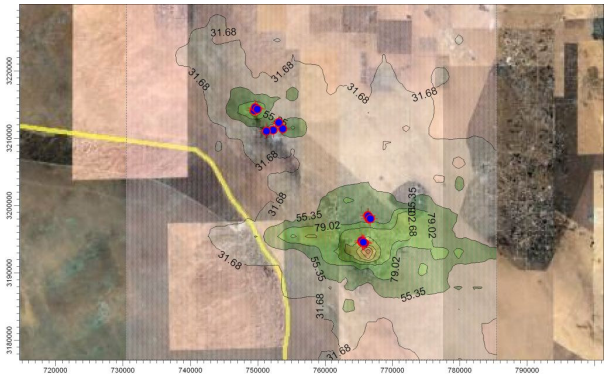

Fig. 13a: Isopleths plot for the maximum hourly average ground level concentrations of methane in µg m^{-3}

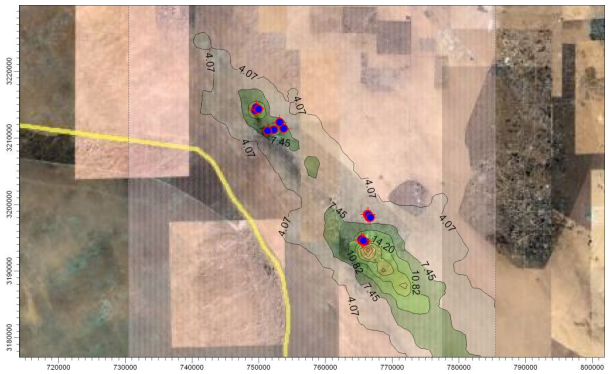

Fig. 13b: Isopleths plot for the maximum hourly average ground level concentrations of methane in µg m^{-3}

Organic Compounds). However the methane and non-methane hydrocarbons gases provide typical samples which can be used as an input for the ISCST3 model to investigate of the effects of emission from flaring in all Kuwait Oilfields

- There is a need for an emission inventory strategy for KOC to minimize the impact of methane and non-methane hydrocarbons released from flaring activities

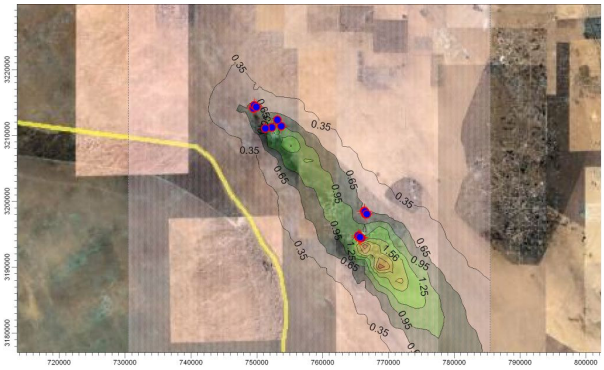

Fig. 13c: Isopleths plot for the maximum annual average ground level concentrations of methane in µg m^{-3}

MODEL PERFORMANCE

The performance of the model is evaluated based on the comparison of 50 highest daily measured and predicted concentrations of methane and non-methane hydrocarbons from KOC flaring at each monitoring station. The overall conclusion of this comparison is that the model predictions are in good agreement with the observed data with accuracy of 60-94% at the monitoring stations used by Kuwait EPA.

CONCLUSION

The simulation of real hourly air quality in the State of Kuwait for the year 2006, inserting the source emission data for that year into the ISCST3 software indicates that the levels of methane and non-methane hydrocarbons from flaring activities in NK Oilfields exceed the allowable daily ambient air standard set by Kuwait EPA.

The model prediction show that these green house gas levels are as much as 248.49 and 3099.8 µg m^{-3} above the accepted KAAQS for methane and non-methane hydrocarbons, respectively.

Overall, the statistical comparison between the 50 highest daily measured and predicted concentrations at Kuwait existing monitoring sites shows that the model is in good agreement with the observed data.

This study can be extended to include other pollutants such as NO_X, SO_2, CO, CO_2 and the organic components. Therefore, there is a need for a proper emission inventory strategy for KOC to minimize the impact of NO_X, SO_2, CO, CO_2, methane and non-methane hydrocarbons released from flaring activities.

ACKNOWLEDGMENT

The researchers would like to thank Kuwait Oil Company for the field data used in this study and their permission to publish the results. Also, the authors would like to thank the Environmental Public Authority of Kuwait and Kuwait International Airport for the field data used in this study.

REFERENCES

1. Khaireyah, Kh. AL-Hamad and A.R. Khan, 2007. Total emissions from flaring in kuwait oilfields. ISSN 1553-345X© 2007 Science Publications. Am. J. Environ. Sci., 4 (1): 31-38.
2. US Environmental Protection Agency, 1999. PCRAMMET User's Guide (Revised). EPA-454/R-96-001. Office of Air Quality Planning and Standards, Research Triangle Park, North Carolina 27711.
3. US Environmental Protection Agency, 1995. User guide for the industrial source complex (ISC3) dispersion models. Volume I, User Instructions. EPA-450/B-95-003a. Research Triangle Park, N.C: Environmental Protection Agency. Office of Air Quality Planning and Standards, Emissions, Monitoring and Analysis Division.
4. US Environmental Protection Agency, 1992. User guide for the industrial source complex (ISC) dispersion models. EPA-450/4-92-008A. Research Triangle Park, N.C: Environmental Protection Agency. Office of Air Quality Planning and Standards.
5. Holzworth, G.C., 1972. Mixing heights, wind speeds and potential for urban air pollution throughout the contiguous United States. Office of Air Prog. pub. AP-101,USEPA, RTP, NC.
6. Hanna, S.R., 1969. The thickness of the planetary boundary layer. Atmos. Environ., 3: 519-536.